Interaction of iron with the local environment in SiGe alloys investigated with Laplace transform deep level spectroscopy

Vl. Kolkovsky,[1] A. Mesli,[2] L. Dobaczewski,[1] N. V. Abrosimov,[3] Z. R. Żytkiewicz,[1] and A. R. Peaker[4]
[1]*Institute of Physics, Polish Academy of Science, Warsaw, Poland*
[2]*Institut d'Electronique du Solide et des Systèmes, CNRS/ULP, Strasbourg, France*
[3]*Institute of Crystal Growth, Berlin, Germany*
[4]*Centre for Electronic Materials Devices and Nanostructures, University of Manchester, Manchester, United Kingdom*
(Received 22 May 2006; published 9 November 2006)

Laplace transform deep level transient spectroscopy (LDLTS) is used to investigate the alloy effects on iron related deep centers in $Si_{1-x}Ge_x$. A clear buildup of alloy disorder as a function of the germanium content has been observed for the isolated interstitial iron. However, due to specific features of the interstitial tetrahedral position of iron in the cubic lattice, it is not possible to say how many Ge atoms are responsible for the alloy-induced level splitting of the electronic state of the interstitial iron related defect. The observation of alloy splitting for the iron-boron pair has been used to resolve this issue. Different shells of nearest-neighbor atoms form the alloy pattern for both the interstitial isolated iron and the iron-boron pair. We show that for the iron-boron pair the occupied state is formed when a hole is closer to iron in the case of low germanium content. For more germanium rich alloy compositions the hole is bound by boron resulting in a dramatic change in the LDLTS peak structure. In an attempt to simulate the observed patterns, the alloying effects originating from different shells containing the defect were considered. A clear tendency for iron to form a pair with boron siting in germanium rich neighborhood is demonstrated. Finally, the influence of alloying on iron motion has been investigated. Similarities in the dissociation potential barrier heights of the iron-boron pair in pure silicon and $Si_{0.98}Ge_{0.02}$ alloy suggest that the presence of Ge atoms induces only a second-order effect on the average diffusion barrier in alloys with low Ge content (less than 3%).

DOI: 10.1103/PhysRevB.74.195204 PACS number(s): 71.55.Cn, 68.55.Ln, 72.20.Jv

I. INTRODUCTION

The interest in silicon-germanium ($Si_{1-x}Ge_x$), a fully miscible solid solution, has shown a significant increase in recent years owing to its many applications in microelectronic and optoelectronic devices. These results form the ability to produce devices with unique properties due to the band gap and lattice parameter variation as the composition is changed.[1,2] The material has existing and future promise in high-frequency applications such as SiGe heterojunction bipolar transistors, passive inductors, capacitors, and transmission line elements. The successful technological application of such $Si_{1-x}Ge_x$ structures is inseparably linked to a fundamental understanding of their microscopic properties. Among these one of the most important is an understanding of the electronic properties of the lattice defects. Point defects in such alloys are quite sensitive to the local atomic environment and, as a result, the underlying electrical and optical properties depend on whether the nearest neighbor atoms are Si or Ge. Such alloy effects have been observed for various impurities in $Si_{1-x}Ge_x$. In addition, alloying induced local atomic disorder and band gap shrinkage, two major properties of the alloy, lead to serious deviations from what is known in pure silicon. We may cite the role played by local atomic arrangements upon elastic properties of the vacancy,[3] hydrogen atoms in the bond center position,[4] the *A*-center,[5] and some transition metals and their complexes.[6–9]

Due to its high diffusivity, iron may easily be introduced into silicon-based materials during heat treatment. This results in a deterioration of device properties (see, e.g., Ref. 10 for more details). Moreover, in *p*-type materials the positively charged iron atoms are attracted by negative shallow acceptors forming the well-known iron-acceptor pairs, enhancing the effective solubility of iron and modifying its electronic properties. There are many reports concerning the presence of iron in pure silicon but only a few groups have investigated the iron related complexes and its electrical properties in SiGe alloys. Mesli *et al.*[7] showed that neither iron nor iron-boron electronic levels are pinned to the conduction or the valence band. These levels move towards the valence band much faster than the shrinkage of the band gap with increasing Ge content. On the other hand, a loss of symmetry of the deep level transient spectroscopy (DLTS) peaks has been observed with an increase of the Ge content. The shoulders responsible for the loss of symmetry have been assigned to unknown defects which could not be investigated in detail because of the poor resolution of the conventional DLTS technique.[7] Two other groups have concentrated attention on the behavior of isolated iron atom in SiGe crystals, its microscopic details[11] and the energy level position.[12] In previous work[9] we have shown that applying high-resolution Laplace DLTS (Ref. 13) allows the alloying effects originating from different shells of atoms surrounding the point defect to be investigated in detail. This has been done for the case of Au,[6] Pt,[6] and Fe (Ref. 9) atoms in $Si_{1-x}Ge_x$. The alloy disorder observed around these defects made it possible to conclude about the most likely host atoms arrangements in the neighborhood. This implies for a given impurity atom some siting preference in the $Si_{1-x}Ge_x$ lattice. In this work we concentrate our attention on the alloy effects for isolated iron and its complexes in the $Si_{1-x}Ge_x$ crystals restricting our study to low Ge concentrations. The

observed alloy-induced electronic level splitting effects for the isolated and paired iron are related to the well known microscopic structures of both forms of this metal atom. The observed patterns in the Laplace DLTS signals are compared to the results of simulations where the alloying effects originating from different shells of atoms surrounding the defect are taken into account. Finally, the possible influence of the alloy effect on the iron-boron pair stability and dissociation is discussed in detail.

II. EXPERIMENTAL PROCEDURE

Samples for this study were prepared from *p*-type unstrained B-doped $Si_{1-x}Ge_x$ $(0<x<0.071)$ crystals which were grown by the Czochralski technique in argon atmosphere. The alloy compositions were measured by Rutherford backscattering. The boron concentration ranged from 1×10^{14} to 3.5×10^{15} cm^{-3}. Highly pure iron (99.9999%) was scratched on one side of the wafers and diffused at 950 °C in an argon atmosphere followed by quenching in liquid N_2 in the expectation that a significant amount of iron would remain on interstitial sites and avoid precipitation. Schottky barriers were fabricated by thermal evaporation of aluminum dots. Following this procedure only the energy level at $E_V+0.1$ eV related to the iron-boron pair has been observed in the DLTS spectra because of association of the positive interstitial iron with the negative acceptor during the Schottky processing. In order to dissociate this complex and observe the isolated interstitial iron, the samples were heated at 360 K for 60 min. During this procedure the Schottky barrier was biased with −9 V in order to establish the neutral charge state of iron so preventing the Coulombic attraction between iron and negatively charged boron. This *in situ* annealing procedure leads to the formation of the isolated interstitial iron centers whose DLTS fingerprint is a donor level located at $E_V+0.43$ eV.

III. RESULTS AND DISCUSSION

Figures 1 and 2 show the Laplace DLTS spectra for the iron donor center and the iron-boron pair in relaxed SiGe crystals with 0–7.1% of Ge. Usually, the isothermal Laplace DLTS spectra are presented on a frequency scale. However, because of our interest in the alloy-induced shift of iron-related energy levels, the frequency scale of these graphs has been converted into an energy-difference in the following way: $\Delta E=-k_BT\times\ln(e_n/e_{n0})$, where e_n is the emission rate value on the original spectrum, ΔE is the energy value on the rescaled graph, and e_{n0} is a reference frequency (here the frequency of the corresponding peak observed in pure silicon). It is worth emphasizing that rescaling graphs in such a way needs to assume that the capture cross sections of both interstitial Fe_i and Fe_iB_s are not affected by the Ge content.[7] The spectra have been normalized in terms of magnitude and were shifted vertically so as to be ranked in order of the germanium content in the samples. Clearly there is no structure for germanium-free (pure silicon) crystals and we have dominant sharp lines both for the Fe_iB_s pair and the interstitial Fe_i. This is in agreement with a monoexponential hole

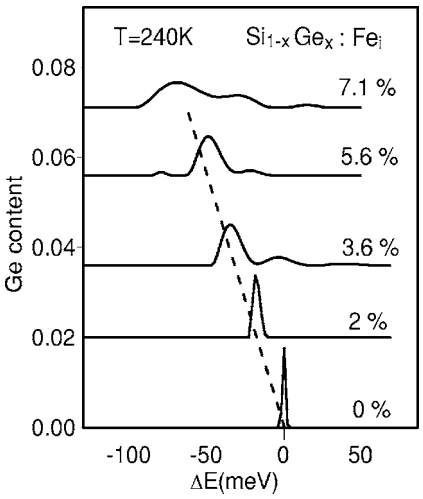

FIG. 1. Laplace DLTS spectra observed for the interstitial isolated iron in $Si_{1-x}Ge_x$ $(0<x<0.071)$. The usual frequency scale has been converted into energies according to the procedure described in the text. The vertical shift of the spectra is proportional to the germanium content in the crystal. The dashed line connects the centers of gravity of the main peak in each of the spectra demonstrating the linear alloy shift of this peak.

emission process expected from well-defined single energy levels. The increase of Ge content causes the additional satellite peaks to appear in the Laplace DLTS spectra forming a structure (called a pattern hereafter) on both sides of the dominant line. Moreover, for both cases these dominant lines become broader and shift on the energy scale towards lower values, i.e., the energy related levels move closer to the valence band with the addition of Ge atoms into the Si lattice.

The additional peaks observed in the Laplace DLTS spectra for the isolated interstitial iron Fe_i and for the iron-boron pair Fe_iB_s can be related to the presence of different local environments around each defect in the alloy. In previous

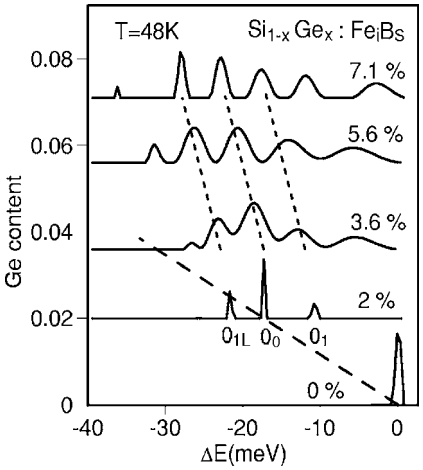

FIG. 2. Laplace DLTS spectra observed for the iron-boron pair in $Si_{1-x}Ge_x$ $(0<x<0.071)$. This figure has been prepared in a similar way to Fig. 1. The dashed line represents the same alloy shift as the one shown in Fig. 1. The dotted line connects the centers of gravity of the main peaks observed for the 3.6%, 5.6%, and 7.1% Ge samples.

studies of other defects in SiGe the impact of the local alloy configuration on defect energy levels has been interpreted as a change of the chemical nature of host atoms surrounding the defect.[6] Following the original picture proposed in the pioneering paper by Ludwig and Woodbury,[14] iron behaves as a free ion in silicon with no direct bonds to the host atoms. However, this simple picture, although generally accepted, does not permit a straightforward interpretation of the present observations. The donor level of the isolated interstitial iron originates from one of the *d* orbitals of the iron split by the crystal field and interacting with the atomic orbitals of the surrounding silicon atoms. If one of the host silicon atoms surrounding the interstitial tetrahedral position, where the iron atom sits, is replaced by a germanium atom then some of individual bond lengths change and, obviously, the chemical identity of this host atom changes as well. As a result, the electronic level of iron shifts increasing its energy separation from the valence band (the subsidiary peaks in Fig. 1 due to the alloy appearing on the right-hand side of the main peak). The energy difference between the electronic levels of iron siting in different local alloy configurations is called the alloy splitting effect. Yonenaga *et al.*[15] showed that in the SiGe alloys the individual Si-Si and Si-Ge distances change much less than the average distance between the host atoms (given by the Vegard's law). As a result, one can expect that the alloy splitting effect does not change much within the range of the alloy compositions investigated in this study. Figure 1 confirms this statement as the main and subsidiary peaks remain at the same distance from each other.

The ionic model of the iron-boron pair and related electronic level[16] predicts that the electrostatic potential of the charged acceptor shifts the electronic levels of the interstitial iron upwards in the energy scale. Thus the double donor state of iron emerges from the silicon valence band and this level, when combined with a single negative charge of an acceptor, is seen as a single donor state of the pair. Therefore, the physical reasons why one observes the alloy effect for the iron-boron pair can be twofold. First, due to a modification of the atomic-like level splitting by the crystal field mentioned above. Second, the replacement of one silicon atom by germanium results in a modification of the iron-boron distance leading to a shift of the iron energy level due to a modified Coulombic potential experienced by iron from the acceptor. Similarly to the case of the isolated iron and based on the observations by Yonenaga *et al.*, one can come to a similar conclusion that the magnitude of the alloy splitting for the iron-boron pair does not change much with the alloy composition.

The iron and boron atoms can also form more distant pair giving rise to a metastable configuration which, according to the ionic model, should result in the electronic level being closer to the valence band.[17] However, in our experiments no metastable form of the Fe_iB pair has been observed over the whole range of Ge content. This fact may seem to be inconsistent with previous results obtained by Dobaczewski *et al.*[17] who observed the dissociation of the Fe_iB pair after a moderate electron injection into the depletion layer followed by the electron-hole recombination. This discrepancy could be explained by the fact that the minority carrier injection

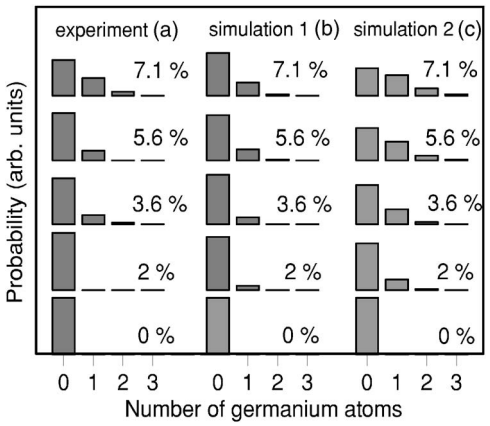

FIG. 3. The amplitudes (integrated areas) of the Laplace DLTS peaks (a) compared to probabilities of finding a given number of germanium atoms in the first-nearest neighborhood of the metal for a random alloy with different Ge content for two different cases: (b) four nearest neighbors forming the alloy pattern assuming the six more distant atoms do not contribute to the pattern; (c) ten nearest equivalent neighbors and eight atoms in the second shell. The detailed structures for these two cases are shown in Fig. 4.

followed by the recombination process, transferring some of the energy to the recombination center, i.e., the Fe_iB pair, is a dynamic process and the relative concentrations of the close and more distant pairs are governed by a much slower kinetics process. Thus, in our experiments even though the more distant pairs may form during the annealing process, its steady-state concentration may not be large enough to be observed. It is worth remembering that, at least in pure silicon, to establish the metastable configuration, special cooling procedures are required.[16] Such procedures were not followed in the present study.

The complex structures observed in Figs. 1 and 2 do not allow us to assign unambiguously a particular peak to a specific alloy configuration around the defect in a similar way to the case of substitutional gold and platinum in SiGe.[6] Figure 3(a) shows a flat diagram of the Laplace DLTS peak amplitudes which has been calculated numerically as areas under each peak observed on the spectra. These experimental values are compared in Figs. 3(b) and 3(c) representing the simulations for two different alloy configurations, each involving a different number of host atoms possibly influencing the isolated iron electronic level. The interstitial tetrahedral site in the diamond structure has four nearest neighbors, six second neighbors (distant by only 14%), and eight neighbors at twice the distance of the nearest ones (see Fig. 4 for details). The first case displayed in Fig. 3(b) assumes that only the four nearest atoms have a major influence on the interstitial iron energy level. In the second case displayed in Fig. 3(c), we consider a shell formed by the first- and the second-nearest neighbors. As stated above, these ten atoms are almost equally distant to iron and could thus have a similar influence on its energy level. The horizontal scales for both diagrams [Figs. 3(b) and 3(c)] denote the number of germanium atoms influencing the interstitial iron energy level and, by analogy, a similar meaning is attributed to the horizontal scale of Fig. 3(a) representing the experimental

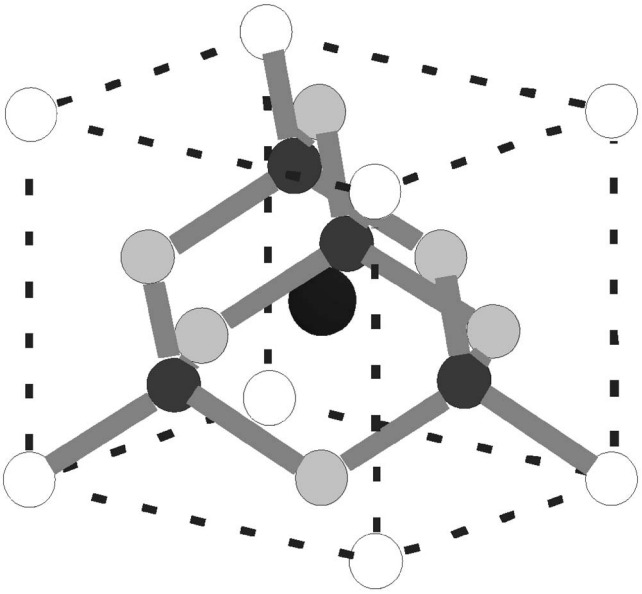

FIG. 4. Atomic structure surrounding the interstitial tetrahedral isolated iron (the central large atom). The four small black atoms are the nearest. Six gray atoms form the second shell; slightly more distant (by 14%) than the atoms forming the first shell. The third shell is formed by the eight white atoms which are located at twice the distance of the nearest ones.

data. The experimental patterns observed in Figs. 1 and 2 and the simulations carried out following the procedure outlined above seem to favor the case where only the four nearest host atoms affect the iron energy level. However, as one can see in the spectra corresponding to isolated iron (Fig. 1), the peaks broaden indicating that even though the four nearest atoms have the strongest impact on the iron energy level, more distant atoms also play some important role in the alloy effect. Thus, in reality, the experimental observations reflect a situation somewhere intermediate between the models represented by simulations in Figs. 3(b) and 3(c).

In a previous study we have successfully treated the case of gold and platinum, two species known to occupy the substitutional site.[6] The effects of the first and second neighbors could be unambiguously distinguished as the atomic distances involved are clearly different. In the present case of iron the situation is more complex as discussed above. Thus a clear distinction between the first and second shells cannot be made without ambiguity so weakening any conclusion on the preferential environment of iron. Consequently, comparing the experimental diagram [Fig. 3(a)] with the results of simulation of the first case where only the first shell plays a key role [Fig. 3(b)] one could conclude that a germanium rich environment is preferred by interstitial iron. This effect is seen for the 7.1% Ge sample if one compares the relative experimental and simulated amplitudes corresponding to the one-germanium atom peak and the no-germanium peak. On the other hand, if we take into account both the first and second shells [Fig. 3(c)] then we come to the opposite conclusion, i.e., that a preference for a germanium rich environment surrounding iron would be unlikely.

Due to the horizontal axes rescaling in Figs. 1 and 2, one can directly compare the magnitudes of the alloy effects observed for Fe_i and Fe_iB. The numerical procedures used for the Laplace transform inversion calculate the total amplitude and the position on the horizontal scale of the center of gravity of each peak observed in the spectrum. The energy distances between the main and the first small peak on the right-hand side for the spectra shown in Fig. 1 for the 3.6%, 5.6%, and 7.1% alloys are similar and are around 40 meV which is the magnitude of the alloy splitting effect observed for Fe_i. For Fe_iB (see Fig. 2 and the spectrum for the 2% alloy) this distance is around 7 meV. These large values allow us to conclude that in both cases there has to be a substantial difference in the distance between atoms responsible for the alloy effect and the defect. This conclusion can be supported by a recent study of platinum in SiGe alloy layers.[6] A similar but slightly smaller difference in the magnitude of the alloy effect originating from the first and second shell around platinum has been reported. As a result, we can safely claim that for the Fe_iB pair the alloy effect, which is much weaker on the energy scale than for Fe_i, is caused by host atoms much more distant from iron. By analogy with the platinum case,[6] we assign the labeling 0_0, 0_1, etc. to the main peaks of the structures belonging to Fe_iB. The main number corresponds to the number of germanium atoms in the first shell and the subscript is the number of germanium in the second shell for a given alloy configuration. Following the ionic model, we can attribute the observed energy separation between the peaks 0_0 and 0_1 to the alloy induced change of the iron-boron distance. According to the ionic model, the energy separation of these two peaks (around 7 meV) divided by the pair binding energy (around 520 meV)[15] should scale with the relative change of the iron-boron distance (shortening by about $7/520 \approx 1.3\%$) when one of the silicon atoms in the second nearest shell is replaced by a germanium atom. Similarly for the alloy effect for Fe_i, the configurations involving more germanium atoms around Fe_iB should be represented by subsequent peaks on the right-hand side of the main line. However, the striking feature observed in the case of Fe_iB is that a line appears on the left-hand side of the main peak which cannot be explained by the concept of the ionic model described above. The labeling 0_{1L} is assigned to this line whose interpretation is discussed in further paragraphs.

The activation energies extracted from Arrhenius treatment of the emission rates of the iron-boron pair and interstitial iron are given in Table I. In this table the label 0_0 is assigned to the main peak corresponding to the Fe_iB pair in Si and SiGe whereas the peaks on its right- and left-hand sides are labeled 0_1 and 0_{1L}, respectively. It is worth noting that the spectra observed for Fe_iB pair in SiGe with Ge concentrations higher than 5% become quite broad with more satellite lines. In consequence the Arrhenius-type analysis becomes inconclusive. This difficulty has already been met in the cases of the VO center, and of Au and Pt related defects in SiGe alloys.[5,6] In all these instances it was very difficult to obtain stable and reliable high-resolution DLTS spectra for alloy compositions higher than 5%. As seen in Table I (upper), the data are consistent with the shifts of Fe_i-related peak reported in Fig. 1. Similarly, the shift of Fe_iB-related peak when the Ge content is increased from 0 to 2% Ge is consistent with the absolute values of the ioniza-

TABLE I. The activation energies for thermal emission of the main and some subsidiary lines in the Laplace DLTS spectra for the interstitial iron donor center (upper) and its pair with boron (lower) in different SiGe alloy compositions. The lines, for which reliable Arrhenius plots could not be obtained, are marked by n/o.

Alloy composition (% of Ge)	Main peak
0	436±6 meV
2	420±6 meV
3.6	410±3 meV
5.6	382±12 meV

Alloy composition (% of Ge)	Main peak 0_0	Peak 0_1	Peak 0_{1L}
0	100±2 meV		
2	85±2 meV	97±2 meV	79±2 meV
3.6	82±12 meV	n/o	n/o

tion energies obtained from the Arrhenius analysis [see Table I (lower) and Fig. 2].

The dashed line in Fig. 1 joins the centers of gravity of the main peaks through all spectra demonstrating that the energy level of Fe_i shifts linearly with the germanium content in the range of the alloy compositions considered. The dashed line in Fig. 2 starts at the center of gravity of the peak for pure silicon and has the same slope as the dashed line in Fig. 1 (notice that the energy scale differs in the figures). Similar alloy slopes have been observed by Mesli *et al.*[7] using conventional DLTS. However, a discontinuity is clearly seen in Fig. 2. The dashed line joins the centers of gravity of the 0_0 emission lines for the samples corresponding to germanium concentrations of 0% and 2% but misses the dominant peaks in the remaining three spectra. The striking feature is that if the dashed line representing the 0_0 emission from Fe_iB for 0% and 2% Ge is extrapolated to higher Ge content, a resonance of this level with the valence band would follow which is clearly not what we observe. The main peaks for alloy compositions larger than 2% are joined by a set of parallel dotted lines having a slope radically different from the dashed line joining the peaks related to 0% and 2%.

In general, both Fe_i and Fe_iB levels would be expected to have the same or very similar alloy shifts over the range studied for two main reasons. First, transition metal behavior in $Ga_{1-x}Al_xAs$ alloys led to the conclusion that on an absolute energy scale (indexed to the average dangling bond energy) the iron-related energy levels do not change with the alloy composition.[18] Second, according to the ionic model the Coulombic interaction between iron (Fe^+) and the acceptor (B^-) modifies the energy level for the isolated iron (corresponding to the transition $Fe^{0/+}$) by an amount in principle independent of the alloy composition. As stated above the $(Fe^+B^-)^{0/+}$ pair represents actually the double donor level of iron ($Fe^{+/++}$) which in the absence of Coulombic interaction (in intrinsic or *n*-type material) is buried in the valence band. As a result, for both configurations of iron, i.e., isolated or paired, the iron atom binds the hole responsible for the observed capture-emission processes. We would thus expect both transitions, $Fe^{0/+}$ and $(Fe^+B^-)^{0/+}$ or equivalently $Fe^{+/++}B^-$, to shift with the same slope with increasing Ge content.

It is clearly seen in Fig. 2 that the dotted lines joining the iron-related peaks in samples containing more than 2% of Ge have distinctly different slopes than for lower Ge content. It should be emphasized here that the low-temperature signals observed in the samples with a large Ge content clearly originate from iron-boron pairs because they have very similar stabilities and are affected by annealing in exactly the same way as those observed in 0% and 2% samples. These facts suggest that in the crystals with more germanium the paired iron atom is not able to bind the hole due to the fact that its state becomes resonant with the valence band. The isolated boron is a shallow acceptor, however when it is accompanied by iron its energy must deepen by ~50 meV, and it is this deepened boron state that can be attributed to the iron-boron energy state for larger alloy compositions. Apparently, this change in the hole binding structure does not affect the pair formation process and its stability is still appropriately described by the ionic model.

A similar effect has been observed in silicon carbide whose polytypes correspond to stable configurations differing only in the stacking sequence of periodic Si-C double layers along the *c* axis. As in any Si-based material, a group-III atom substituting for silicon acts as an acceptor since there is a deficit of one valence electron to complete the normal tetrahedral bonding. In cubic 3C and hexagonal 4H and 6H polytypes, boron provides a first shallow acceptor state at 0.3 eV above the valence band as measured by Hall effect and admittance spectroscopy. At the same time, a second acceptor boron center, introducing a deeper level into the band gap with an activation energy about 0.65 eV, has been observed by some groups.[18–20] The origin of this deeper boron related acceptor level is uncertain and whether it corresponds to a deepening of the first shallow level caused by a nearby defect is still disputed. It has been suggested that it is connected with boron replacing a carbon atom (B_C).[19] Other groups proposed that this level is associated with a boron atom replacing a silicon atom with an adjacent carbon vacancy or an antisite with silicon in the carbon position.[20,21] It is believed that in the SiGe alloys, boron can act as a deeper defect under the influence of Fe_i and Ge possibly explaining our observations. Following this scheme one can postulate a scenario for the behavior of the Fe_iB pair in SiGe alloys. For a Ge content lower than 2% the hole is trapped by Fe_i whereas for larger alloy compositions the hole is trapped by boron. The change in the alloy patterns observed in Fig. 2 should reflect this transformation in the hole localization making a direct comparison of the two series of patterns meaningless. In particular, it would be difficult to extract any relevant information on the alloy disorder around Fe_iB. Thus, we will focus on the analysis of the alloy effect in each case separately. The energy distances between the peaks observed for Fe_i and Fe_iB in the sample with 2% of Ge lead us to conclude that in the case of isolated Fe_i the host atoms of the first shell are responsible for the alloy effect whereas those of the second shell merely make the Laplace DLTS peaks broader only. In the case of the Fe_iB pair the alloy effect due

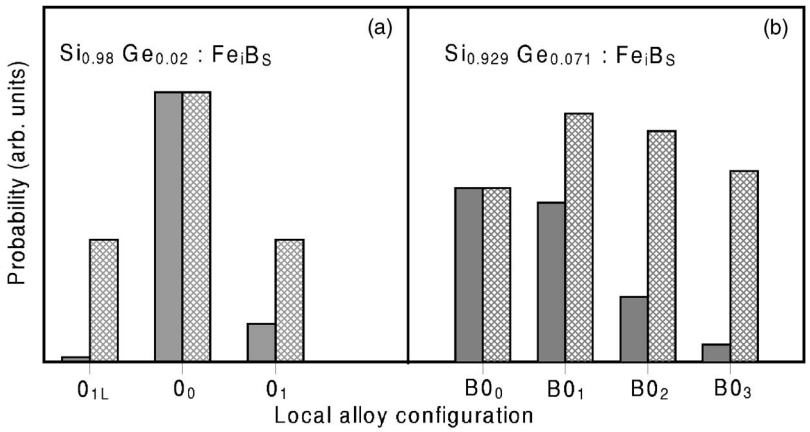

FIG. 5. Simulation analysis (dark gray color) showing the probabilities of finding a given local alloy configuration in the second-nearest neighborhood around the Fe_iB pair (see text for details). In (a) we consider the interstitial iron in $Si_{0.98}Ge_{0.02}$ and in (b) boron in $Si_{0.929}Ge_{0.071}$ (b). The experimental results are shown as light gray bars.

to the first shell cannot be observed. The pattern seen in the spectra is caused by more distant atoms. As a result, for the $Si_{0.98}Ge_{0.02}$ sample it is assumed that the peak on the right-hand side labeled 0_1 in Fig. 2 corresponds to no germanium atoms among the nearest host atoms and one germanium in the second-nearest shell. All the eight second-nearest sites seem to be equivalent except the one which lies on the $\langle 111 \rangle$ direction which is the pair axis. The presence of the germanium atom in this particular position may form a different shift of the Fe_iB electronic level and, as a result, can be responsible for the peak 0_{1L} located on the left-hand side in Fig. 2.

The probability of finding a given number of germanium atoms in the second-nearest neighborhood around the Fe_iB pair in the random SiGe alloys is shown in Fig. 5(a) (dark gray bars). The configuration with one germanium in this shell of atoms has been divided in the ratio of 1:7 among the configurations of 0_{1L} and 0_1 to account for the fact (mentioned above) that the eight second-nearest sites are not equivalent when dealing with the Fe_iB pair. In this figure the light gray bars represent the amplitudes of the Laplace DLTS peaks observed in the sample with 2% Ge. The experimental and simulated amplitudes for the 0_0 configurations are normalized. It is clearly seen that the experimental amplitudes of the 0_1 and 0_{1L} configurations are much larger than the ones obtained from the simulation. A similar diagram is displayed in Fig. 5(b) for $Si_{0.929}Ge_{0.071}$, however in this case a different model has been employed. Here it has been assumed that the alloy pattern is related to the substitutional boron atom and the peaks observed in the spectra represent the alloy effect in the second-nearest shell surrounding the substitutional boron. These configurations are distinguished from the previous ones by applying the symbols $B0_0$, $B0_1$, etc. In this case, there should not be any configuration equivalent to 0_{1L} and a small peak on the left-hand side of the spectrum is ignored. Similarly in the case of Fig. 5(a), the experimental amplitudes are drawn in Fig. 5(b) and from this diagram it is seen that there is a very strong preference for the defect to form in the germanium rich environment as well.

Based on a common picture of the formation process of the iron-acceptor pairs one should not expect to see any iron-boron pair siting preference. The driving force for the pair formation is a long-range Coulombic attraction between the negatively charged acceptor and positively charged iron atom. By using the procedure presented in Ref. 22, one can evaluate that in the temperature range where the pair forms the capture radius of mobile iron by immobile boron is about 5 nm. For our doping levels (1×10^{14} to 3.5×10^{15} cm^{-3}) the average distance between boron atoms is larger than the capture radius by at least an order of magnitude, in consequence the individual capture radii do not overlap. The pair formation process is thus totally random.

In general, one can observe certain iron-boron pair siting preference if the total energy of the pair is lower for boron being surrounded by some particular alloy configuration. However, from the simple ionic model, based on the point charge concept, a diffusing iron atom will not be influenced by this as its migration is unaffected by the particular alloy configuration in the nearest neighborhood of the closest boron atom. On the other hand, as seen in Fig. 5(b) an obvious iron siting preference has been detected. We believe therefore, that at short distances, the simple Coulombic model is not appropriate. Thus the local potential resulting from the atomic environment determines the pair total energy and constitutes the driving force for pairing with a specific boron atom siting in a preferential alloy environment. This is despite the fact that, as it has been shown by Hattendorf *et al.*,[23] boron itself does not show any siting preference in SiGe.

This preference is possible if the pair does not form in a single pairing process. Namely, at the forming temperatures the iron atom may be trapped by any boron according to the ionic model but finds itself thermodynamically less stable than with another boron atom with which the pair total energy is lower because that boron atom is in a Ge rich environment. In that case the iron atom leaves the less favorable boron to seek a more stable one. In other words, the large capture radius does not stop the pair formation process being controlled by thermodynamic constraints.

In the third part of this study we concentrate on the way the motion of interstitial iron is affected by adding germanium atoms into the silicon lattice. The diffusion of iron depends on the height of the energy barrier separating two adjacent lattice sites. In the case of a long range diffusion process and because of randomness, this barrier height should be well-averaged over all visited sites. The fact that in the Laplace DLTS spectra different alloy configurations around the Fe_iB pair are observed, a study of the dissociation

process is expected to provide us with more quantitative information on the thermal stability of these configurations and thus on the alloy effect itself. The analysis of the spectra discussed above led us to the conclusion that the observed hole transitions involve iron ($Fe^{+/++}$) only in Si and $Si_{0.98}Ge_{0.02}$. Therefore, our discussion of the dissociation kinetics described below is restricted to these two materials. The pair dissociation process takes place in the 300–400 K range, i.e., at temperatures where free interstitial iron is significantly mobile. In the frame of the ionic model the time constant of the dissociation kinetics of the Fe_iB pair is governed by the activation energy for dissociation required for Fe_i to be detached from the pair and brought several lattice distances away. The corresponding dissociation time constant is described by the following equation:

$$\tau_{diss} = (1/\nu)\exp[E_{diss}/(k_B T)], \quad (1)$$

where ν is the attempt frequency of the process.

In this work the dissociation process of the Fe_iB pair has been examined in sequences of isochronal annealing steps at different temperatures. After each step the sample was quickly cooled to the measurement temperature (around 47 K for iron-boron pair and 240 K for isolated interstitial iron) and the concentrations of both the Fe_iB pair and interstitial Fe_i were measured using the Laplace DLTS technique. In order to avoid pair formation during the cooling and warming procedures, a large reverse bias is applied after each isochronal annealing step, keeping the charge state of iron neutral. All iron existed as iron-boron pairs before starting any annealing series. Figure 6 shows the dissociation kinetics of the Fe_iB pair in both pure silicon and $Si_{0.98}Ge_{0.02}$ crystals as a result of a series of isochronal annealing steps. The dissociation barriers E_{diss} have been determined directly from the corresponding Arrhenius plots shown in Fig. 7.

In silicon we find a dissociation barrier of 1053 meV. This result is consistent with the one obtained by Feichtinger[24] (1170 meV). In $Si_{0.98}Ge_{0.02}$ we find very similar values for both 0_0 and 0_1, respectively 1025 meV and 1000 meV. The slight difference between the latter values is within the experimental uncertainty and thus cannot be related to the alloying. Iron diffuses in silicon between equivalent interstitial sites, thus the energy barrier governing this process should be extremely sensitive to distances between host atoms. Adding germanium into the alloy expands the lattice on average but the individual Si-Si and Si-Ge bond lengths do not change. For an alloy with a small composition change as it is the case with 2% of germanium one does not expect any percolation paths for iron diffusion. Only very few iron jumps occur close to germanium and they can be faster than the other ones. As a result, one can expect that the presence of germanium in such diluted SiGe alloys have only a second-order effect on the averaged diffusion barrier. On the other hand, the presence of germanium close to the iron-boron pair may have some particular influence on the iron-boron pair stability by modifying the barrier for the first jump of the iron atom being very close to the charged acceptor where the coulombic interaction is the strongest.

After each annealing step the increase of the isolated interstitial iron Fe_i concentration has been monitored as well. It

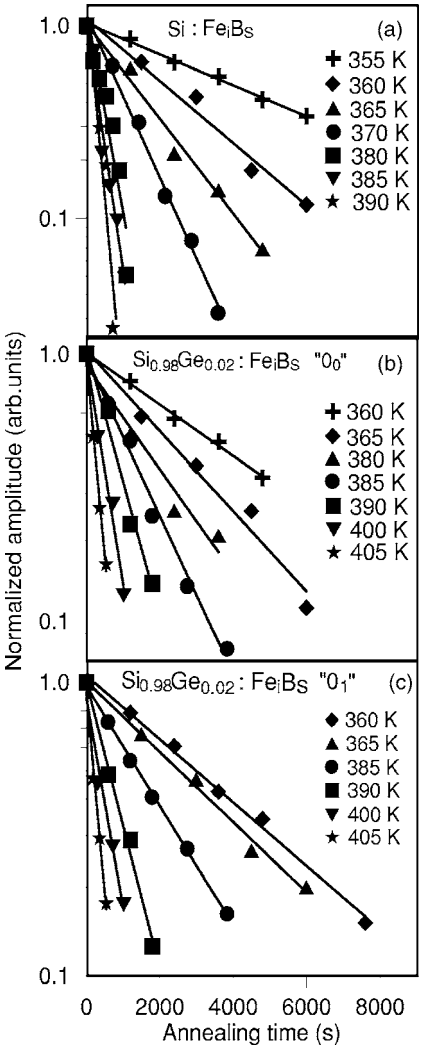

FIG. 6. The Fe_iB dissociation kinetics measured as a decrease of the Laplace DLTS peak amplitude (a) in pure Si and in $Si_{0.98}Ge_{0.02}$ for two main peaks: "0_0" (b) and "0_1" (c). The dissociation time constants are 3, 5, 7, 17, 28, 44, and 90 min for Si crystal and for $Si_{0.98}Ge_{0.02}$ are 5, 9, 15, 25, 37, 49, 76 min (b) and 5, 10, 15, 30, 62, 72 min (c).

allowed us to obtain independently the values of 1088 meV for Si and 1118 meV for $Si_{0.98}Ge_{0.02}$. The similarity in the rates, and consequently in the barriers, obtained from the iron-boron pair dissociation and the growth of the isolated iron signal suggest that there are no intermediate states with significant concentrations participating in the pair dissociation. This clearly suggests that the same microscopic process is responsible for the pair dissociation and the growth of the isolated iron. The reverse preexponential factor in the Arrhenius-equation (1), which represents the attempt frequency of the interstitial iron atom during its passage over a classical potential barrier, was found to be about 5×10^{11} s^{-1}. This value is very close (within the accuracy of its evaluation) to the range of 10^{12}–10^{13} s^{-1} attributed to the lattice vibration frequency and this fact confirms that a single iron jump is the iron relocation process in the crystal between adjacent unit cells.

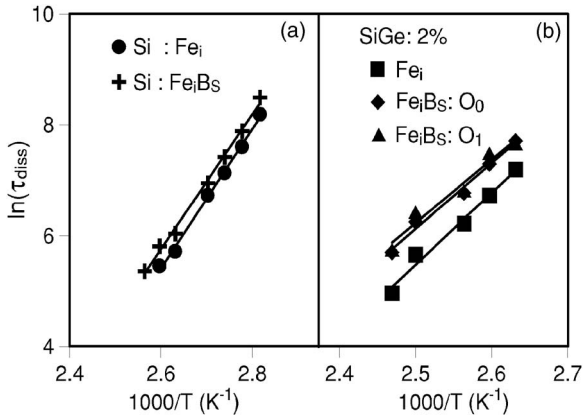

FIG. 7. Arrhenius plots of τ_{diss} versus $1000/T$ extracted from the data of Fig. 6 in Si (a) and $Si_{0.98}Ge_{0.02}$ (b) for the FeB pair (two main configurations 0_0 and 0_1 in $Si_{0.98}Ge_{0.02}$). These plots are compared to the Arrhenius plots of the interstitial isolated Fe_i signal appearance observed in the same experiment.

IV. SUMMARY

The high resolution Laplace DLTS technique has been used to demonstrate the alloy effects on iron related deep centers in relaxed bulk $Si_{1-x}Ge_x$ samples. For the isolated interstitial iron a clear buildup of the alloy disorder as a function of the germanium content has been observed, however, it is not possible to attribute a specific atomic arrangement to the electronic level of the iron. This is due to specific features of the interstitial tetrahedral position of iron in the cubic lattice. The observations of the alloy effect on the iron-boron pair has allowed us to conclude that different shells of nearest neighbors play the key role in the formation of the alloy pattern. We have shown that for iron-boron pair the occupied state is formed when a hole is trapped by iron in low germanium contents leading to the transition $Fe^{+/++}$. For larger alloy compositions the hole is bound by boron ($B^{-/0}$) resulting in a dramatic change in the alloy peak pattern. Comparing the observed patterns of the Laplace DLTS peaks with the simulations that take into account different shells of atoms around the defect, a clear tendency for iron to form a pair with boron sites in the germanium rich neighborhood is demonstrated. Finally, the influence of Ge atoms in the silicon lattice on iron motion has been investigated. Similarities in dissociation potential barrier heights of the iron-boron pair in both pure silicon and $Si_{0.98}Ge_{0.02}$ alloys suggest that the influence of Ge atoms on the average diffusion barrier in alloys with low (less than 3%) Ge content is negligible.

ACKNOWLEDGMENTS

This work has been financially supported in Poland in part by the Ministry of Scientific Research and Information Technology Grant No. 3T08A02126 and in the UK by the Engineering and Physical Sciences Research Council.

[1] H. G. Grimmeiss, Semiconductors **33**, 939 (1999).
[2] B. S. Meyerson, Sci. Am. **270**, 42 (1994).
[3] A. Mesli and A. Nylandsted Larsen, Phys. Rev. Lett. **83**, 148 (1999).
[4] K. Bonde Nielsen, L. Dobaczewski, A. R. Peaker, and N. V. Abrosimov, Phys. Rev. B **68**, 045204 (2003).
[5] V. P. Markevich, A. R. Peaker, J. Coutinho, R. Jones, V. J. B. Torres, S. Öberg, P. R. Briddon, L. I. Murin, L. Dobaczewski, and N. V. Abrosimov, Phys. Rev. B **69**, 125218 (2004).
[6] L. Dobaczewski, K. Gościński, K. Bonde Nielsen, A. Nylandsted Larsen, J. Lundsgaard Hansen, and A. R. Peaker, Phys. Rev. Lett. **83**, 4582 (1999); K. Gościński, L. Dobaczewski, K. Bonde Nielsen, A. Nylandsted Larsen, and A. R. Peaker, Phys. Rev. B **63**, 235309 (2001).
[7] A. Mesli, B. Vileno, C. Eckert, A. Slaoui, C. Pedersen, A. Nylandsted Larsen, and N. V. Abrosimov, Phys. Rev. B **66**, 045206 (2002).
[8] A. Mesli, P. Kringhøj, and A. Nylandsted Larsen, Mater. Sci. Forum **258-263**, 145 (1997).
[9] VI. Kolkovsky, A. Mesli, L. Dobaczewski, N. V. Abrosimov, Z. R. Żytkiewicz, and A. R. Peaker, J. Phys.: Condens. Matter **17**, S2267 (2005).
[10] A. A. Istratov, H. Hieslmair, and E. R. Weber, Appl. Phys. A: Mater. Sci. Process. **70**, 489 (2000).
[11] M. Hoehne, U. Juda, J. Wollweber, D. Schulz, J. Donecker, and A. Gerhardt, Mater. Sci. Forum **196-201**, 359 (1995).
[12] K. Nauka and T. I. Kamins, Physica B **273-274**, 603 (1999).
[13] L. Dobaczewski, A. R. Peaker, and K. Bonde Nielsen, J. Appl. Phys. **96**, 4689 (2004).
[14] G. W. Ludwig and H. H. Woodbury, in *Solid State Physics: Advances in Research and Applications*, edited by H. Ehrenreich, F. Seitz, and D. Turnbull (Academic Press, New York, 1962), Vol. 13, p. 223.
[15] I. Yonenaga, M. Sakurai, M. Nonaka, T. Ayuzawa, M. H. F. Sluiter, and Y. Kawazoe, Physica B **340-342**, 854 (2003).
[16] A. Chantre and D. Bois, Phys. Rev. B **31**, 7979 (1985).
[17] L. Dobaczewski, Z. Wilamowski, and M. Surma, in *Proceedings of* 23rd *International Conference on the Physics of Semiconductors, Berlin, 1996*, edited by M. Scheffler and R. Zimmermann (World Scientific, Singapore, 1996), p. 2705.
[18] J. M. Langer, C. Delerue, M. Lannoo, and H. Heinrich, Phys. Rev. B **38**, 7723 (1988).
[19] M. Bockstedte, A. Mattausch, and O. Pankratov, Mater. Sci. Forum **353**, 447 (2001).
[20] A. v. Duijn-Arnold, T. Ikoma, O. G. Poluektov, P. G. Baranov, E. N. Mokhov, and J. Schmidt, Phys. Rev. B **57**, 1607 (1998).
[21] B. Aradi, A. Gali, P. Dèak, E. Rauls, Th. Frauenheim, and N. T. Son, Mater. Sci. Forum **353-356**, 455 (2001).
[22] A. A. Istratov, H. Hieslmair, and E. R. Weber, Appl. Phys. A: Mater. Sci. Process. **69**, 13 (1999).
[23] J. Hattendorf, W.-D. Zeitz, W. Schröder, and N. V. Abrosimov, Physica B **340-342**, 858 (2003).
[24] H. Feichtinger, Acta Phys. Austriaca **51**, 161 (1979).